ChemComm

COMMUNICATION

View Article Online
View Journal | View Issue



Cite this: *Chem. Commun.*, 2017, 53, 1864

Received 19th December 2016,
Accepted 18th January 2017

DOI: 10.1039/c6cc10083j

www.rsc.org/chemcomm

# Self-assembly, self-sorting, and electronic properties of a diketopyrrolopyrrole hydrogelator†

Emily R. Draper, Bart Dietrich and Dave J. Adams*

**We show here the first example of a hydrogel formed from a symmetrically functionalised diketopyrrolopyrrole aromatic core. Gelation is triggered by change in pH. Not only does this gelator form aggregated, entangled structures at low pH, but it also forms worm-like micelles at high pH. The structures at high pH can be aligned using shear to provide conductive materials.**

Gelation is a powerful and versatile method of self-assembly.[1,2] Not only can this self-assembly approach be used to provide frameworks for cell culture and differentiation,[3–5] it is now also being used for the optimisation of organic electronics, and materials for water splitting.[6–8] This wide use of gels now means that even more structures with different functionalities are being investigated with the aim of self-assembling them into single and multicomponent systems. Gelation itself results from the self-assembly of low molecular weight gelators (LMWG) into fibres. At a suitable concentration, there are sufficient fibres to form an entangled network.

Gelation using a slow pH change has proved a useful tool to prepare reproducible hydrogels, as well as to induce self-sorting of differently functionalised gelators.[9–15] For example, we have recently shown a self-sorted system of a p-type gelator and an n-type gelator.[16] If the HOMO/LUMO levels match up, this results in a p–n heterojunction where the self-assembled p-type fibres meet the n-type self-assembled fibres.[17] p–n heterojunctions are the important component of many electronic devices such as OPVs and transistors. There are now many examples of n-type gelators being used to form hydrogels, for example perylene bisimides and naphthalene bisimides.[1,2,6] A number of p-type gelators have been described, including tetrathiafulvalene, oligophenylvinylene, and oligothiophene based gelators.[18–22] However, there is still a need to develop new examples to expand the potential for optoelectronic systems.

Diketopyrrolopyrroles (DPPs) are an example of an electron-rich material that have been widely used in solar cells and other electronic applications.[23–28] These molecules have the ability to carry holes that can be tuned by altering substituent groups on the pyrrolopyrrole core.[29] The planarity of the core makes for favourable π stacking and orbital overlap optimising charge transport through the material.[30,31] There are examples of DPPs being used as polymers, crystalline materials and organogels.[24,32–35] Using LMWG allows a high degree of self-assembly as well as ease of synthesis and processability.

A DPP that is capable of self-assembling to form an organogel has recently been illustrated by Thool *et al.*[32] The organogel was formed *via* a heat-cool method. Here, we show to the best of our knowledge the first example of a DPP which is capable of self-assembling in water to give a hydrogel. We are able to form a gel in water using a slow pH drop method. The resulting gels can be used in a photoconductive system.

**DPP-1** (Fig. 1a) was synthesised using established procedures.[29] First, the core was formed by base-catalysed condensation of two equivalents of thiophene-2-carbonitrile onto dimethyl succinate, with the succinate backbone forming the core bridgehead. The bilateral linker tags were installed *via* $S_N2$ reaction of the core with *tert*-butyl chloroacetate, followed by acid-mediated deprotection of the *tert*-butyl ester.

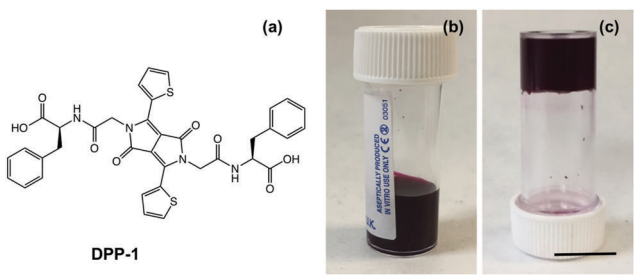


Fig. 1 (a) Molecular structure of **DPP-1**; (b) photograph of a solution of **DPP-1** at pH 8 and a concentration of 5 mg mL$^{-1}$; (c) photograph of a gel of **DPP-1** at pH 3.3 formed by lowering the pH of the solution shown in (b). The scale bar represents 1 cm.

*School of Chemistry, Joseph Black Building, College of Science and Engineering, University of Glasgow, Glasgow, G12 8QQ, UK. E-mail: dave.adams@glasgow.ac.uk*

† Electronic supplementary information (ESI) available: Synthetic procedures and analysis, SEM images, neutron scattering. See DOI: 10.1039/c6cc10083j

Finally, the resulting diacid was coupled with *tert*-butyl L-phenylalaninate using standard peptide coupling methodology, followed by acid-mediated deprotection of the *tert*-butyl ester. By functionalising with phenylalanine, the carboxylic acid on the amino acid could be used to solubilise the molecule at high pH as well as drive self-assembly upon protonation.

Hydrogels of **DPP-1** were formed by dissolving the gelator at 5 mg $mL^{-1}$ in water using 1 molar equivalent of 0.1 M NaOH and leaving to stir overnight to ensure that the gelator had dissolved fully. This resulted in a free flowing dark pink solution at pH 8 (Fig. 1b). UV-vis absorption spectra in solution showed relatively broad peaks even when diluted (Fig. S1, ESI†) with the most intense peaks at 500 nm and 530 nm. Viscosity measurements also suggested the presence of structures in solution that shear thin upon increasing shear rate (Fig. S2a, ESI†). SEM of dried solutions using 1 molar equivalent of NaOH showed ill-defined structures which could have resulted from drying (Fig. S3b, ESI†). When 2 molar equivalents of NaOH were used to prepare the solution of **DPP-1**, the resulting solutions showed no shear thinning behaviour implying that there are very few or very small structures present in solution (Fig. S2b, ESI†). Since we are aiming to prepare films of self-assembled one-dimensional aggregates, the samples prepared with two equivalents of NaOH are therefore unsuitable and were not pursued further.

Gelation was then triggered by adding 5 mg $mL^{-1}$ of glucono-$\delta$-lactone (GdL) to the solution of the DPP. The slow hydrolysis of GdL leads to a homogenous drop in pH to 3.3 that resulted in reproducible gelation of the sample (Fig. 1c).[9,36] Rheological measurements showed that the **DPP-1** gel at pH 3.3 has a storage modulus ($G'$) of $\sim$900 Pa and a loss modulus ($G''$) of $\sim$90 Pa, typical of a gel formed by a LMWG. Strain sweeps revealed the gels start to break at 10% strain (Fig. S4a, ESI†), and show slight frequency stiffening at higher frequencies in the frequency sweeps (Fig. S4b, ESI†). At this point, SEM images of the dried gel show a randomly orientated fibrous network with fibre widths of on average 30 nm (Fig. S3a, ESI†), which is again typical for such gels. The gelation kinetics could be followed using rheology and monitoring the pH during gelation; this is possible due to the slow hydrolysis of GdL (Fig. S5a, ESI†).

Gelation started to occur after 8 minutes, as shown by an increase in $G'$ and $G''$; the pH at this point had reached 7.3. There was then a second increase in $G'$ and $G''$ at 30 minutes at pH 4.5. The sample completely gelled by 400 minutes, where values of both $G'$ and $G''$ plateau. At this point, the pH has stopped decreasing at a pH of around 3.3. The p$K_a$ of the terminal carboxylic acids of the **DPP-1** was measured to be around 7.3 at 25 °C (determined by the dropwise addition of dilute acid).[37] Once the pH was lowered below that of the p$K_a$, then gelation started to occur (Fig. S5b, ESI†). This is consistent with our other work on related gelators. The p$K_a$ value is important when using multi-component systems to ensure self-assembly can occur of the different components (see below).[10–12,16]

Solutions and gels of **DPP-1** were dried into thin films using a mask of fixed dimensions to give samples with a thickness of between 2–3 μm based on previous data using the same 3 × 3 mm mask and 10 μL of sample.[38] The UV-vis absorption spectra showed a red shift and broadening of the peaks for both the dried solution and the xerogel, suggesting that the samples are H-aggregated as compared to the equivalent hydrated samples (Fig. 2a). This was also observed by Golwaki *et al.* when drying hydrated samples onto glass.[39] The thin films were then examined using cross-polarised light microscopy. Both the xerogel and the dried solution showed no anisotropy, implying that no crystallisation had occurred whilst drying and forming the thin films (Fig. S6, ESI†).

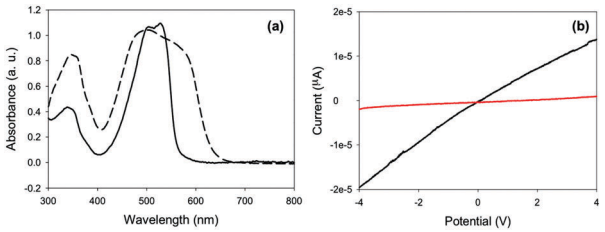


Fig. 2 (a) UV-vis absorption spectra of **DPP-1** xerogel (dashed line) and in solution (0.04 mg $mL^{-1}$, solid line). (b) *I–V* curves of **DPP-1** xerogel (black line) and dried solution (red line).

The resistivity of the dried solutions and xerogels was then measured to determine whether they could be used in organic electronic devices. *I–V* curves revealed that the xerogel was less resistive than the dried solution (Fig. 2b), but both materials showed ohmic contact. The higher conductivity of the xerogel could be due to a greater alignment in the material so making the movement of the current easier, or potentially a different molecular packing in the gel state.[31]

To test whether **DPP-1** was suitable to be used in a conductive device, the resistivity of both the dried solution and xerogel of **DPP-1** were again measured. The samples were then doped by exposure to a vapour of iodine for 20 minutes to allow diffusion into the thin films.[40–42] The resistivity was then re-measured and the resistivity had decreased, showing the **DPP-1** film was able to reduce the iodine and therefore lower the resistance of the film (Fig. 3a and b).

The xerogel was more effective than the dried solution, as it showed a much greater decrease in resistance in the presence of iodine. When left in air, allowing the iodine to diffuse out from the films, the current returned to that as before iodine was added.

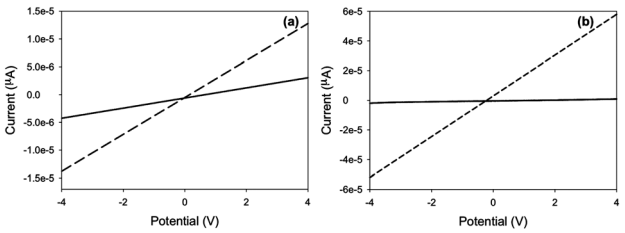


Fig. 3 (a and b) Show *I–V* of the resistivity of samples before the addition of iodine vapour (solid line) and after being exposed to iodine vapour for 20 minutes. (a) Shows data for the dried solution and (b) shows data for the xerogel.

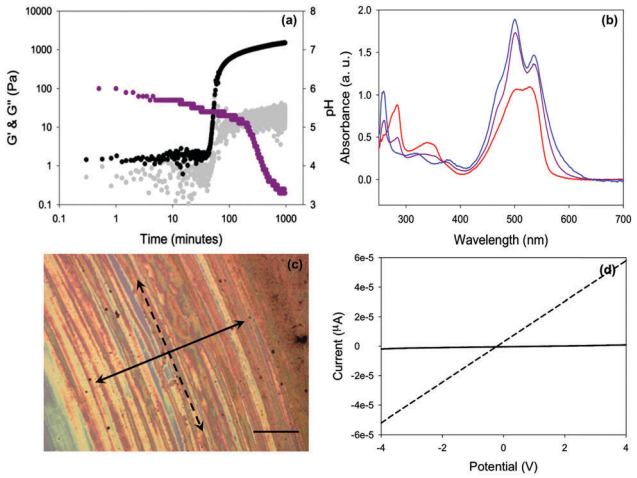


Fig. 4 (a) Monitoring gelation of **DPP-1** + **PBI-A** with the development of $G'$ (black data) and $G''$ (grey data) over time with the decrease in pH (purple data) (b) UV-vis absorption spectra of **DPP-1** (red data), **PBI-A** (blue data) and **DPP-1** + **PBI-A** (purple data) gels (c) polarised optical microscopy image of a shear aligned dried solution of **DPP-1**. Scale bar represents 0.2 mm. (d) *I*–*V* curves showing the resistance with alignment (dashed line in both (c) and (d)) and against alignment (solid line in both (c) and (d)).

With this positive electron scavenger data, **DPP-1** was then co-assembled with a perylene-based LMWG (**PBI-A**, Fig. S7, ESI†), a known n-type gelator.[38,43] From previous work, both the solution and xerogel of **PBI-A** are only responsive to UV light.[38,43] The introduction of an electron-rich gelator should shift the wavelength dependence of the system into the visible region, due to less energetic wavelengths of light being needed to cause a response. We have recently shown this is the case using a stilbene-based p-type gelator.[16] Here, self-sorting of the **DPP-1** and **PBI-A** was shown to occur by rheology and pH change (Fig. 4a and Fig. S8, ESI†), pH change (Fig. S9, ESI†), UV-vis absorption spectroscopy (Fig. 4b) and NMR spectroscopy (Fig. S10, ESI†). The rheology, pH and NMR studies show that the two different gelators assemble at different times with the **PBI-A** gelling at pH 5.4 after 200 minutes with a sharp decrease in pH after this. The **DPP-1** starts to gel after 8 minutes, as it does alone, and has almost become NMR invisible by the time **PBI-A** has started to gel. The UV-vis absorption spectra of the mixed system compared to those of the single components look like an addition of the two spectra rather than new peaks being present which would occur in a co-assembled system. All these data indicate self-sorting behaviour as we have shown in our previous work,[11,12,16] but we cannot rule out a small amount of co-assembly is occurring. A small amount of co-assembly would be difficult to detect or quantify due to the behaviour of the system being dominated by self-sorting.

Compared to the data for **PBI-A** alone, the wavelength response slightly shifted towards the visible with an increase in response at 400 nm and 470 nm in comparison to the response at 365 nm in the mixed system (Fig. S11, ESI†). However, the current produced from the self-sorted xerogel was significantly lower than that of the **PBI-A** xerogel alone (Fig. S12, ESI†). There are examples in the literature where these kinds of systems do work well, for example by Shinkai and co-workers.[17] We hypothesise that our system does not work as well as other systems as a result of the band-gap overlap not being optimal, or due to the different gelator fibres being intimately mixed resulting in recombination of charges. This intimate mixing would make the sample unsuitable for p–n heterojunctions as it would not be efficient. There is some evidence from SEM that this may be the case, as twisted fibres were observed (Fig. S13, ESI†), but the data are not conclusive and hence is the subject of ongoing research. Finally, the amino acids may be acting as insulators.

We hypothesised that the alignment within the dried solution could be improved since there are worm-like micelles present in solution. We have previously shown that drying a solution which contains worm-like micelles under shear gives aligned structures.[44] Hence, a sample of the **DPP-1** solution was subjected to a shear of 10 rad $s^{-1}$ for 16 hours until the solution had dried. Under cross-polarised light microscopy, the material now showed bright anisotropic structures demonstrating that there was a significant degree of alignment (Fig. 4c and Fig. S14 ESI†). When the resistance was measured along the direction of the alignment (dashed direction in Fig. 4c), there was a much greater conductivity than against the alignment (solid line, Fig. 4d). This can be rationalised by the current being able to more easily pass along aligned structures as there is a shorter path for electrons to travel and so less chance of recombination. Efforts to align the gel were unsuccessful due to the high $pK_a$ and faster gelling times than previous examples.[44] This resulted in the gel being damaged under the shear.

In conclusion, we have shown the first example of a DPP-based low molecular weight hydrogelator. Gels can be formed by slowly lowering the pH, which leads to reproducible homogeneous gels, and also allows us to form multi-component self-sorted systems. This gives the chance to add a n-type gelator with accessible orbitals to be used in conjunction with **DPP-1** to give a p–n heterojunction. The use of water also makes the gels cheaper and environmentally friendly. Both the xerogel and dried solution of **DPP-1** show ohmic contact with the xerogel being less resistive, again showing they could be used in organic electronics. We have also shown we can further process this material to give aligned structures that show directional dependence and improve the conductivity of the material. Finally, the **DPP-1** xerogel and solution can become conductive on the addition of iodine. In a self-sorted system, the use of **DPP-1** as an electron donor was effective in shifting the wavelength response, but resulted in lower absolute currents.

DA thanks the EPSRC for a Fellowship (EP/L021978/1), which also funded ED and BD. The NMR spectrometers used for this work were funded by the EPSRC (EP/K039687/1 and EP/C005643/1). We thank to Matthew Wallace for collection of NMR data in Fig. S12, ESI.†

## Notes and references

1 S. S. Babu, V. K. Praveen and A. Ajayaghosh, *Chem. Rev.*, 2014, **114**, 1973–2129.
2 F. Wurthner, *Chem. Commun.*, 2004, 1564–1579.
3 E. V. Alakpa, V. Jayawarna, A. Lampel, K. V. Burgess, C. C. West, S. C. J. Bakker, S. Roy, N. Javid, S. Fleming, D. A. Lamprou, J. Yang,

A. Miller, A. J. Urquhart, P. W. J. M. Frederix, N. T. Hunt, B. Péault, R. V. Ulijn and M. J. Dalby, *Chem*, 2016, **1**, 298–319.
4 S. Khan, S. Sur, C. J. Newcomb, E. A. Appelt and S. I. Stupp, *Acta Biomater.*, 2012, **8**, 1685–1692.
5 L. Latxague, M. A. Ramin, A. Appavoo, P. Berto, M. Maisani, C. Ehret, O. Chassande and P. Barthélémy, *Angew. Chem., Int. Ed.*, 2015, **54**, 4517–4521.
6 S. S. Babu, S. Prasanthkumar and A. Ajayaghosh, *Angew. Chem., Int. Ed.*, 2012, **51**, 1766–1776.
7 N. J. Hestand, R. V. Kazantsev, A. S. Weingarten, L. C. Palmer, S. I. Stupp and F. C. Spano, *J. Am. Chem. Soc.*, 2016, **138**, 11762–11774.
8 A. S. Weingarten, R. V. Kazantsev, L. C. Palmer, M. McClendon, A. R. Koltonow, P. S. SamuelAmanda, D. J. Kiebala, M. R. Wasielewski and S. I. Stupp, *Nat. Chem.*, 2014, **6**, 964–970.
9 D. J. Adams, M. F. Butler, W. J. Frith, M. Kirkland, L. Mullen and P. Sanderson, *Soft Matter*, 2009, **5**, 1856–1862.
10 E. R. Draper, E. G. B. Eden, T. O. McDonald and D. J. Adams, *Nat. Chem.*, 2015, **7**, 848–852.
11 C. Colquhoun, E. R. Draper, E. G. Eden, B. N. Cattoz, K. L. Morris, L. Chen, T. O. McDonald, A. E. Terry, P. C. Griffiths and L. C. Serpell, *Nanoscale*, 2014, **6**, 13719–13725.
12 K. L. Morris, L. Chen, J. Raeburn, O. R. Sellick, P. Cotanda, A. Paul, P. C. Griffiths, S. M. King, R. K. O'Reilly and L. C. Serpell, *Nat. Commun.*, 2013, **4**, 1480.
13 J. Raeburn and D. J. Adams, *Chem. Commun.*, 2015, **51**, 5170–5180.
14 D. J. Cornwell, O. J. Daubney and D. K. Smith, *J. Am. Chem. Soc.*, 2015, **137**, 15486–15492.
15 J. S. Foster, J. M. Żurek, N. M. S. Almeida, W. E. Hendriksen, V. A. A. le Sage, V. Lakshminarayanan, A. L. Thompson, R. Banerjee, R. Eelkema, H. Mulvana, M. J. Paterson, J. H. van Esch and G. O. Lloyd, *J. Am. Chem. Soc.*, 2015, **137**, 14236–14239.
16 E. R. Draper, J. R. Lee, M. Wallace, F. Jackel, A. J. Cowan and D. J. Adams, *Chem. Sci.*, 2016, **7**, 6499–6505.
17 K. Sugiyasu, S.-i. Kawano, N. Fujita and S. Shinkai, *Chem. Mater.*, 2008, **20**, 2863–2865.
18 A. Ajayaghosh and V. K. Praveen, *Acc. Chem. Res.*, 2007, **40**, 644–656.
19 S. J. George and A. Ajayaghosh, *Chem. – Eur. J.*, 2005, **11**, 3217–3227.
20 A. M. Sanders, T. J. Magnanelli, A. E. Bragg and J. D. Tovar, *J. Am. Chem. Soc.*, 2016, **138**, 3362–3370.
21 A. M. Castilla, M. Wallace, L. L. Mears, E. R. Draper, J. Doutch, S. Rogers and D. J. Adams, *Soft Matter*, 2016, **12**, 7848–7854.
22 W.-W. Tsai, L.-s. Li, H. Cui, H. Jiang and S. I. Stupp, *Tetrahedron*, 2008, **64**, 8504–8514.
23 M. Stolte, S.-L. Suraru, P. Diemer, T. He, C. Burschka, U. Zschieschang, H. Klauk and F. Würthner, *Adv. Funct. Mater.*, 2016, **26**, 7415–7422.
24 M. Grzybowski and D. T. Gryko, *Adv. Opt. Mater.*, 2015, **3**, 280–320.
25 D. Ley, C. X. Guzman, K. H. Adolfsson, A. M. Scott and A. B. Braunschweig, *J. Am. Chem. Soc.*, 2014, **136**, 7809–7812.
26 M. A. Naik and S. Patil, *J. Polym. Sci., Part A: Polym. Chem.*, 2013, **51**, 4241–4260.
27 O. Wallquist and R. Lenz, *Macromol. Symp.*, 2002, **187**, 617–630.
28 T. Aytun, P. J. Santos, C. J. Bruns, D. Huang, A. R. Koltonow, M. O. de la Cruz and S. I. Stupp, *J. Phys. Chem. C*, 2016, **120**, 3602–3611.
29 L. Huo, J. Hou, H.-Y. Chen, S. Zhang, Y. Jiang, T. L. Chen and Y. Yang, *Macromolecules*, 2009, **42**, 6564–6571.
30 F. Pop, W. Lewis and D. B. Amabilino, *CrystEngComm*, 2016, **18**, 8933–8943.
31 C. Kanimozhi, M. Naik, N. Yaacobi-Gross, E. K. Burnett, A. L. Briseno, T. D. Anthopoulos and S. Patil, *J. Phys. Chem. C*, 2014, **118**, 11536–11544.
32 G. S. Thool, K. Narayanaswamy, A. Venkateswararao, S. Naqvi, V. Gupta, S. Chand, V. Vivekananthan, R. R. Koner, V. Krishnan and S. P. Singh, *Langmuir*, 2016, **32**, 4346–4351.
33 P. Sonar, T. R. B. Foong and A. Dodabalapur, *Phys. Chem. Chem. Phys.*, 2014, **16**, 4275–4283.
34 I. Meager, R. S. Ashraf, C. B. Nielsen, J. E. Donaghey, Z. Huang, H. Bronstein, J. R. Durrant and I. McCulloch, *J. Mater. Chem. C*, 2014, **2**, 8593–8598.
35 Y. Patil, R. Misra, F. C. Chen and G. D. Sharma, *Phys. Chem. Chem. Phys.*, 2016, **18**, 22999–23005.
36 Y. Pocker and E. Green, *J. Am. Chem. Soc.*, 1973, **95**, 113–119.
37 L. Chen, S. Revel, K. Morris, L. C. Serpell and D. J. Adams, *Langmuir*, 2010, **26**, 13466–13471.
38 E. R. Draper, J. J. Walsh, T. O. McDonald, M. A. Zwijnenburg, P. J. Cameron, A. J. Cowan and D. J. Adams, *J. Mater. Chem. C*, 2014, **2**, 5570–5575.
39 E. D. Głowacki, H. Coskun, M. A. Blood-Forsythe, U. Monkowius, L. Leonat, M. Grzybowski, D. Gryko, M. S. White, A. Aspuru-Guzik and N. S. Sariciftci, *Org. Electron.*, 2014, **15**, 3521–3528.
40 S. Yoon, J. Cho, S. H. Yu, H. J. Son and D. S. Chung, *Org. Electron.*, 2016, **34**, 28–32.
41 X. Chen, X. W. Chen and W. G. Deng, *Solid State Commun.*, 1994, **89**, 97–100.
42 S. K. M. Nalluri, N. Shivarova, A. L. Kanibolotsky, M. Zelzer, S. Gupta, P. W. J. M. Frederix, P. J. Skabara, H. Gleskova and R. V. Ulijn, *Langmuir*, 2014, **30**, 12429–12437.
43 J. J. Walsh, J. R. Lee, E. R. Draper, S. M. King, F. Jäckel, M. A. Zwijnenburg, D. J. Adams and A. J. Cowan, *J. Phys. Chem. C*, 2016, **120**, 18479–18486.
44 E. R. Draper, O. O. Mykhaylyk and D. J. Adams, *Chem. Commun.*, 2016, **52**, 6934–6937.